Plasma Chemistry and Plasma Processing (2022) 42:1169–1186
https://doi.org/10.1007/s11090-022-10268-w

ORIGINAL PAPER

Dielectric Barrier Discharge Plasma Deoxidation of Copper Surfaces in an Ar/SiH_4 Atmosphere

Viktor Udachin[1] · **Lienhard Wegewitz**[1] · **Sebastian Dahle**[1,2] · **Wolfgang Maus-Friedrichs**[1]

Received: 21 March 2022 / Accepted: 28 May 2022 / Published online: 23 June 2022

Abstract
Nowadays, cold plasma techniques like dielectric barrier discharge (DBD) plasmas have attracted considerable interest in view of high deoxidation efficiencies as well as relative simplicity of setups. Although DBD plasma deoxidation of copper has been mainly studied in Ar/H_2 mixtures, there is no information on reduction performance of such methods in other protective atmospheres. In this study, the reduction of natively oxidized copper surfaces using a DBD plasma in an Ar/SiH_4 atmosphere at 100 hPa and 20 °C was investigated. The influence of a silane gas on the deoxidation performance was studied by varying the SiH_4 concentration from 0.0 to 0.5 vol%. An addition of a SiH_4 gas to an Ar atmosphere results in the increase of the deoxidation effect of a DBD plasma, so almost all Cu_2O was reduced after 10 s of treatment in 0.1 vol% silane. Surface morphology analysis showed formation of particles after Ar/SiH_4 plasma treatments that can be cleaned from the surfaces by wiping. Additionally, characterization of the plasma phase indicated the presence of SiH^* radicals that likely play a role in the deoxidation effect. Moreover, an elimination of residual oxygen and nitrogen species in Ar by addition of SiH_4 was observed.

Keywords Dielectric barrier discharge · X-ray photoelectron spectroscopy · Copper deoxidation · Argon-silane plasma

Introduction

Copper is a significant material for electronic industries [1, 2]. Nevertheless, air-formed native oxides on the copper surfaces substantially modify the characteristics. It is known that oxidized copper surfaces possess poor mechanic, electrical and adhesive properties in comparison to deoxidized ones [1, 3]. For example, Sawada and colleagues reported that the interfacial adhesion between deoxidized copper and epoxy resin was much stronger in

✉ Viktor Udachin
viktor.udachin@tu-clausthal.de

[1] Clausthal Center of Materials Technology, Clausthal University of Technology, Agricolastraße 2, 38678 Clausthal-Zellerfeld, Germany

[2] Department of Wood Science and Technology, Biotechnical Faculty, University of Ljubljana, Jamnikarjeva Ulica 101, 1000 Ljubljana, Slovenia

comparison to the system with natively oxidized copper [3]. Therefore, the reduction of copper surface oxides and improvements of already existing deoxidation methods attract considerable attention.

Among different techniques, non-thermal plasma reduction of copper oxides demonstrates promising results [4–9]. As it was shown in our previous research [9], few nanometer-thick native oxide layers were almost completely removed from copper surfaces within 20 s of treatment using a dielectric barrier discharge (DBD) plasma in an Ar/H_2 gas at 100 hPa. Such treatments showed efficient reduction of copper oxides at room temperature due to the presence of highly reactive atomic hydrogen radicals (H_α) in the plasma phase, but no change of morphology of surface was observed, which is a major advantage of this technique in comparison to the other methods like thermal annealing [9–11]. Nevertheless, practical implementation of an Ar/H_2 DBD plasma as a deoxidation pre-treatment step in metal fabrication processes might become complicated due to the fact that hydrogen-contained mixtures are not preferable atmospheres in metal processing and manufacturing. This is connected with the possibility of damaging of metals due to the penetration of hydrogen into the material i.e. hydrogen embrittlement, especially at elevated temperatures and during surface deformation [12–14]. So, for the successful Ar/H_2 DBD plasma deoxidation and subsequent manufacturing, the sample must be first placed in an environment with the presence of hydrogen and then in a pure inert gas like Ar, respectively. Such problem can be overcome by performing both deoxidation and metal processing steps in the same suitable atmosphere. Therefore, development of a method that can provide a strong deoxidation effect to metal surfaces in known protective atmospheres is of a big interest.

At the moment, the usage of SiH_4-doped argon or nitrogen gases in different industrial processes is expected to provide considerable improvement of the manufacturing operations in comparison to pure gases, which is mainly connected with a creation of better protective atmospheres with less amounts of oxygen [15–18]. The high oxygen affinity of silane allowed to significantly decrease the oxygen partial pressure to less than 10^{-15} hPa, therefore providing an oxygen-free environment and preventing possible re-oxidation of the material [15–18]. Additionally, it was shown that the deoxidation of steel during high temperature brazing in a SiH_4-doped argon atmosphere (with SiH_4 concentrations from 1 to 100 ppm) showed an enhancement in the deoxidation performance in comparison to the processes in pure Ar or N_2 gases [15]. The gain in deoxidation performance was also linked with an elimination of residual oxygen in the amount of several ppm, which is usually present in inert gases [15–18]. Nevertheless, besides a deoxidation effect, a generation of contaminations like SiO_2 particles as a reaction product was observed [15]. Although the influence of such oxygen-free protective environments on metal manufacturing processes is being intensively studied, there is no information on the possibility of applying of non-thermal plasmas for metal deoxidation in SiH_4-doped atmospheres.

Up to date, non-thermal plasmas in different SiH_4-doped atmospheres have been implemented mainly for the generation of silicon-containing films to be applied in solar cells or thin-film transistors [19–24]. Plasma enhanced chemical vapour deposition (PECVD) processes were investigated in H_2/SiH_4 [20], $H_2/He/SiH_4$ [21], $Ar/H_2/SiH_4$ [22] and $Ar/NH_3/SiH_4$ [23] gas mixtures, by using radio-frequency (RF) or DBD plasmas. It was shown that several nanometer-thick amorphous or crystalline silicon-containing films can be formed within seconds of plasma treatment in the mixtures with concentration of SiH_4 from 0.01% to several volume percent. For example, Yu and colleagues produced hydrogenated amorphous silicon films by using DBD plasma in an H_2/SiH_4 gas at the pressure of 2 hPa with the deposition rate of 0.34 nm/s (for the discharge voltage and frequency of 12 kV and 20 kHz, respectively) [20]. The

structure of the films can be varied by changing gas mixtures, pressures as well as the plasma discharge parameters. That is, Bazinette and colleagues performed experiments with DBD plasmas at atmospheric pressure and showed that the deposition rate of hydrogenated crystalline silicon films can be accelerated with the increase of discharge power [25]. Interestingly, Feitknecht and co-authors characterized high frequency glow discharge plasma in pure SiH_4 with optical emission spectroscopy (OES) and observed SiH* and H_α radicals in the plasma phase that were produced during dissociation of the SiH_4 gas [26]. Whereas SiH^* is mainly considered to play a role in the formation of silicon-containing films, atomic hydrogen radicals H_α are known to be effective in copper deoxidation [9, 26, 27]. Therefore, presence of such reactive species in the plasma phase makes SiH_4 plasmas also practical for metal deoxidation. Nevertheless, the deoxidation effect of non-thermal SiH_4 plasmas on metal surfaces has not been studied at all. Thus, promising effect and on the other hand the lack of information draw attention to the need on investigation of the deoxidation effect of DBD plasma in an Ar/SiH_4 atmosphere.

The current study was performed as part of a project within the collaborative research center Oxygen-free production (SFB1368), in which several working groups investigate the influence of an addition of silane to argon gas on different metal manufacturing processes like coating, welding or rolling. To date, it has been already shown by our colleagues that the efficiency of several metal processing methods can be improved by adding SiH_4 gas to Ar and creating an oxygen-free atmosphere [15, 17, 18]. The aim of our project is to study the deoxidation effect of a DBD plasma method in Ar/SiH_4 mixtures, which, if it works out, can be implemented in the industrial fabrication processes as a promising deoxidation pre-treatment step without exchange of the protective atmosphere in the system. In this study, we present the deoxidation effect of DBD plasma in an Ar/SiH_4 gas on copper native oxide layers at room temperature and 100 hPa. The effect of changing the silane concentration during treatment of a copper surface is discussed and supported by the analysis of chemical state and morphology. Additionally, the plasma is characterized using optical emission spectroscopy.

Materials and Methods

Samples and Preparation

Copper foils with the size of 10×10 mm^2 and a thickness of 1 mm (99.99 + %, Mateck GmbH, Jülich, Germany) were highly polished using a sanding machine (Jean Wirtz TG 250, Germany) with silicon carbide sanding papers and wool cloths for final diamond polishing (Struers GmbH, Hannover, Germany), resulting in the smooth freshly prepared metal surface. After the polishing step, the samples were rinsed with ethanol (96%; Sigma-Aldrich Chemie GmbH, Munich, Germany) in an ultrasonic cleaner (Bandelin electronic GmbH & Co. KG, Berlin, Germany) for 5 min, dried and exposed to an ambient atmosphere for several hours, resulting in formation of few nanometer-thick native oxide layer [9, 28–30]. Then, the samples were analyzed via atomic force microscopy (AFM) and transferred into the ultra-high vacuum (UHV) system, where the X-ray photoelectron spectroscopy (XPS) investigations were performed.

Atomic Force Microscopy

The morphology of the samples before and after plasma treatments were analyzed using an Atomic Force Microscope (Dimension 3100, Veeco Instruments Inc., Santa Barbara, USA). The AFM images were taken in the presence of ambient air at room temperature and atmospheric pressure. Commercial cantilevers (NSC15/Al BS, Micromasch, Wetzlar, Germany) with a spring constant of 40 N/m and a resonance frequency in the range of 325 kHz were used in the measurements. The images were recorded at a line-scan frequency of 0.5 Hz. The analysis of images was performed with the SPIP 6.1.1 software (Image Metrology, Lyngby, Denmark).

X-ray Photoelectron Spectroscopy

The chemical structure of surfaces before and after the plasma treatment was characterized via XPS at room temperature in an UHV apparatus with a base pressure of $3{\cdot}10^{-10}$ hPa using a non-monochromatic Al K_α (1486.6 eV) X–ray source (RS40B1, Prevac, Rogów, Poland). X-ray photons irradiated the surface under an angle of 80° to the surface normal, illuminating a spot with a diameter of several mm. Electrons emitted under an angle of 10° to the surface normal were recorded by a hemispherical analyzer (EA10/100, Leybold GmbH, Cologne, Germany). Survey and detailed spectra were recorded at pass energies of 80 eV and 40 eV, respectively. All XPS spectra are displayed as a function of binding energy with respect to the Fermi level. Additionally, a charge correction was applied to all spectra by referencing the C–C binding to 285.0 eV. For quantitative XPS analysis, photoelectron peak areas were calculated via a Marquardt–Levenberg optimization algorithm using CasaXPS (Casa Software Ltd., Bay House 5 Grosvenor Terrace Teignmouth, TQ14 8NE United Kingdom) with a Shirley-type background and approximated Voigt-type profiles as a product of 0.7 Gaussian and 0.3 Lorentzian. The CasaXPS analysis files for the samples are provided in the published dataset [31].

DBD Plasma Reactor

Plasma treatment of copper samples was carried out in a DBD plasma reactor with gas inlet and pump systems to vary the pressure inside the reactor in the range from 10^{-8} to 10^{3} hPa [9]. The reactor was directly attached to the UHV system for XPS analysis via a bakeable valve, allowing to treat and analyze copper surfaces without exposure to the ambient atmosphere during transfer. Figure 1 shows a schematic representation of the setup used for DBD plasma treatment of copper surfaces. The isolated high voltage (HV) electrode consisted of a sealed quartz glass tube with a wall thickness of approximately 2.4 mm that was filled with brass powder to generate a homogeneous electric field, whereas the metal samples formed the grounded counter-electrode with a discharge gap between quartz tube and sample of about 2 mm [9, 32]. The geometric electrode surface area was approximately 113 mm^2. A pre-commercial high voltage power supply with a sinoidal output signal (PlasmaGreen GmbH, Clausthal-Zellerfeld, Germany) was used to generate 10 kV peak voltage (measured during plasma ignition) at 8.8 kHz pulse repetition rate for the plasma treatments [9]. The amount of power and current that were used in the experiments are 20.0 W and 1.6 A, respectively.

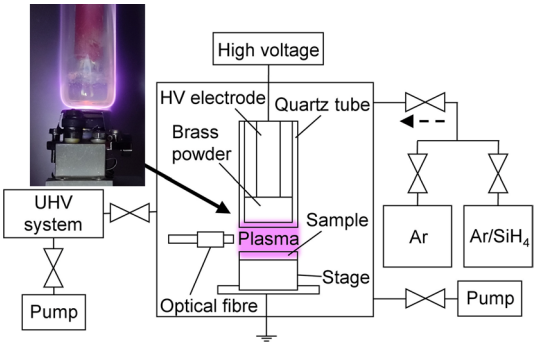

Fig. 1 Schematic representation of the experimental setup. In addition to the schematic representation, a photo of the DBD plasma discharge in an Ar/SiH_4 (0.1 vol%) atmosphere is presented

The samples were treated at a pressure of 100 hPa in Ar 5.0 (Westfalen AG, Münster, Germany) and pre-mixed Ar/SiH_4 gases (Ar 5.0 and SiH_4 4.0 with the concentration of silane of 1.5 vol% in the mixture, Linde GmbH, Pullach, Germany) at room temperature. Creation of working gas atmospheres with different concentration of silane in argon was performed by mixing pure Ar gas with pre-mixed Ar/SiH_4 with the capacitance sensor (Pfeiffer Vacuum GmbH, Asslar, Germany) in the DBD plasma chamber. A photo of the DBD plasma discharge in an Ar/SiH_4 (0.1 vol% of silane) atmosphere, which was taken with a slow-speed camera, is additionally shown in the Fig. 1. The discharge appeared to be uniform.

Plasma Treatment

Before the beginning of the plasma treatment, the reference state of all surfaces was measured with XPS and then the samples were transferred into the plasma chamber. In order to check an impact of a SiH_4 concentration in the working gas mixture on the oxidation state and morphology of copper foils, samples were treated for 10 s at room temperature and 100 hPa and different concentrations of silane. After each experiment, the plasma reactor was evacuated to approx. $5{\cdot}10^{-7}$ hPa and the samples were transferred into the UHV chamber for XPS measurements. The process of pumping and transfer required about 120 s. Additionally, investigation of the reduction kinetics at the lowest possible concentration of SiH_4 in Ar of 0.02 vol% was performed by treating samples at several time intervals until an overall treatment time of 80 s. After each treatment step, the samples were measured with XPS.

Characterization of Deoxidation Effect

In order to be able to compare the deoxidation effects of a DBD plasma in Ar/SiH_4 mixtures with different concentrations of silane, the relative change in stoichiometry of the samples in relation to the reference states as determined with XPS survey analysis for copper, oxygen and carbon specimens was calculated. That is, the relative change in percentage (%) was calculated with the Eq. (1), taking into account the initial concentration of analysed species before treatment ($n_{species(initial)}$) and the concentration of them after a treatment step ($n_{species(after)}$).

$$Relative\ change = \frac{n_{species(after)} - n_{species(initial)}}{n_{species(initial)}} \times 100\% \quad (1)$$

whereas the reference surfaces before treatments did not contain Si and N species, an increase in the amount of Si and N was calculated as an absolute value in atomic percentage (at%), by using the Eq. (2).

$$Absolute\ change = n_{species(after)} - n_{species(initial)} \quad (2)$$

Optical Emission Spectroscopy

Active species within the Ar/H_2 DBD plasma were identified via optical emission spectroscopy (OES) using an AvaSpec–ULS2048CL–EVO fiber-optic spectrometer (Avantes, Netherlands) with a measurement range of 200–1100 nm. In order to detect the emission in the DBD plasma phase, a glass fibre was introduced into the reactor using a vacuum feedthrough (Avantes, Netherlands) (c.f. Fig. 1). Emissions were detected in the beginning of plasma treatments at room temperature. Optical emission spectra were analysed using AvaSoft 8 (Avantes, Netherlands).

Results and Discussion

SiH_4-Doped Ar Plasma Treatment at Different Concentrations of Silane

Table 1 shows the changes in stoichiometry of samples after 10 s plasma treatment at different concentrations of silane in an Ar gas at room temperature. We demonstrate the removal of oxygen as well as carbon species in relation to the reference states with the increase of SiH_4 concentration. That is, pure Ar plasma showed weakest deoxidation and cleaning effects in comparison to SiH_4-doped Ar plasma treatments. As it is mentioned later in the text, a pure Ar plasma effect is mainly connected with the partial removal of adventitious organic contaminations as well as adsorbed water, whereas SiH_4-doped Ar plasma treatments additionally provide reduction of lattice copper oxide. Although deoxidation effect

Table 1 Change in stoichiometry of the samples as determined with XPS for specimens treated in Ar/SiH_4 plasmas with different silane concentrations

Vol% SiH_4	Treatment duration	Relative change in %			Absolute change in at%	
		Cu	O	C	Si	N
0.00	10 s	+ 16	− 14	− 6	0	0
0.02		+ 25	− 23	− 11	+ 2	+ 1
0.05		+ 34	− 37	− 31	+ 7	+ 2
0.10		+ 25	− 45	− 56	+ 14	+ 6
0.50		"Si" film	"Si" film	"Si" film	+ 100	0

For Cu, O and C species a relative change in percentage was calculated, whereas an absolute change in at% was determined for Si and N species

of SiH_4 plasma is efficient, we observe more silicon contaminations on the surface with the increase of SiH_4 concentration (c.f. Table 1; stoichiometry of the surfaces and the corresponding survey spectra are presented in the Table S1 and Figure S1 in supplements, respectively). For example, plasma treatments in Ar/SiH_4 mixtures (0.05 and 0.1 vol%) show formation of Si-containing separated particles, whereas plasma treatment at 0.5 vol. % of silane concentration leads to the formation of > 10 nm thick Si-containing films, such that the Cu substrate could not be detected in XPS anymore (supporting AFM images of the surfaces are presented later in the text). In contrast, a very weak signal from silicon species could be observed with XPS on the surface of the sample that was treated for 10 s in an Ar/SiH_4 (0.02 vol%). Additionally, more nitrogen species were observed with the increase of silane concentration up to 0.1 vol%, which can be linked with the deposition of Si–N on the surfaces [25, 33, 34]. Moreover, presence of nitrogen in the working gas was observed via OES (shown later in the part 3.3), which is known to be a typical contamination in an Ar gas [35]. Therefore, it can be assumed that an addition of silane resulted in the more effective deoxidation of copper surface compared to pure Ar DBD plasma treatment and, in contrast, deposition of mainly Si–O and most probably Si–N species on the surface. Nevertheless, no nitrogen as well as oxygen and carbon species were observed on the surface after 10 s treatment in an Ar/SiH_4 (0.5 vol%) that resulted in a thick not oxidized pure silicon film.

For a better understanding of the nature of the contaminant Si layers, analysis of the Si 2p regions was performed. Figure 2a shows the Si 2p regions of samples after 10 s of treatment in an Ar/SiH_4 plasma with the concentration of silane from 0.02 to 0.5 vol% (shown from bottom to the top) in comparison with the reference sample (bottom spectrum, dark green line). Generally, the Si 2p region of the samples consists of two main components. The first part in the binding energy range from 99 to 101 eV is characterized by a wide Si^0 peak structure [36–39] that can be clearly observed in the spectrum from the samples after treatment in 0.05, 0.1 and 0.5 vol% Ar/SiH_4 mixtures. Due to the known complexity in distinguishing of Si–O and Si–N species in the Si 2p region, the second component in the binding energy range from 101 to 104 eV was assumed to be the superposition of the emissions from different oxidation states of silicon in oxides Si–O and nitrides Si–N (with Si^{1+}, Si^{2+}, Si^{3+} and Si^{4+}) [36–40]. Therefore, 10 s treatments at the concentration of silane from 0.05 to 0.1 vol% led to the formation of pure silicon as well as Si–O and Si–N species on the surface, whereas 10 s treatment in 0.5 vol% Ar/SiH_4 mixture resulted only in the

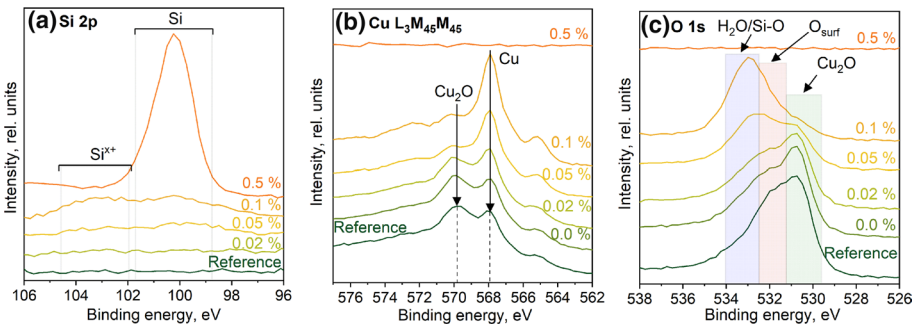

Fig. 2 **a** Si 2p, **b** Cu $L_3M_{45}M_{45}$ and **c** O 1 s regions of the reference sample (bottom dark green line) and after 10 s treatment in pure Ar (green line) and by adding 0.02 vol% (yellow-green), 0.05 vol% (yellow), 0.1 vol% (orange) and 0.5 vol% (dark orange) of SiH_4 to Ar (Color figure online)

deposition of a more than 10 nm-thick pure silicon film. The component Si^{x+} in the region 101–104 eV for the sample after 10 s treatment with the lowest concentration of silane of 0.02 vol% shows a slight increase of intensity in comparison to the reference state that can only be distinguished in the enlarged spectra provided in the supplements (Figure S2). This indicates that this sample was also covered with the minor amount of Si^{x+} species.

The reduction effect of the plasma is presented in Fig. 2b, c. We show the changes in the Cu LMM Auger region (c.f. Fig. 2b) after 10 s treatment in Ar/SiH_4 mixture with the concentration of SiH_4 from 0 to 0.5 vol% (spectra are displayed from bottom to the top) in comparison to the reference state (bottom spectrum, dark green line). The Cu $L_3M_{45}M_{45}$ region after pure argon plasma has almost the same structure as the reference state, showing no sharp increase in the metallic Cu contribution (spectroscopic line at 568 eV) on the surface [9, 28, 41–43]. In contrast to that, even the addition of 0.02 vol. % SiH_4 into the gas mixture provided a decrease of the Cu_2O line (569.8 eV) and an increase of the metallic Cu line. The most efficient reduction of copper native oxide was observed after 10 s plasma treatment in the 0.1 vol. % Ar/SiH_4 mixture, whereas 10 s treatment in 0.5 vol% Ar/SiH_4 atmosphere resulted in a silicon film completely covering the copper surface, so no signal of the Cu LMM line was observed.

The effect of reduction of copper native oxide in Ar/SiH_4 plasmas was observed also in the O 1 s region (c.f. Fig. 2c). Generally, three main components were distinguished in this region: Cu_2O lattice oxide, adsorbed surface oxygen species (OH^-) and water, organic as well as silicon oxide species at 530.5, 531.7 and 532.9 eV, respectively [9, 28, 37, 41, 43–46]. A pure Ar plasma provided a weak cleaning effect, so minor amounts of adsorbed surface oxygen as well as water and organic species were removed. Nevertheless, no decrease of the Cu_2O intensity was observed. In contrast, even small addition of SiH_4 gas provided visible reduction of the Cu_2O native oxide layer, showing almost no copper oxide after treatment in an Ar/SiH_4 (0.1 vol%) atmosphere. At the same time, deposition of Si–O oxide species was observed with the increase of silane concentration. Thus, an addition of SiH_4 to an Ar gas provided an substantial improvement of the deoxidation performance, whereas it can be concluded that pure Ar plasma does not play a significant role in the reduction process of copper native oxides.

Morphology Analysis

The morphology of samples is presented in Fig. 3. As it was shown in our previous research, Ar/H_2 DBD plasma treatment does not affect the surface structure in comparison to the reference state [9]. We observed the same effect on the surface that was treated in an Ar DBD plasma (c.f. Fig. 3a). The surface after treatment in an Ar/SiH_4 gas (0.02 vol%) was found to be covered with a minor amount of particles with diameters of 80 nm (c.f. Fig. 3b) and thickness of approximately 10 nm. With the increase of silane concentration to 0.05 and 0.1 vol%, more bigger particles were observed on the surfaces. For example, the surface of a sample which was treated by a 0.05 vol% Ar/SiH_4 plasma contained separately distributed big clusters with the sizes of 300 nm in diameter and 80 nm thick and smaller particles of 200 nm in diameter. Much more particles but with an equal diameter of approximately 200 nm were observed on the surface after 0.1 vol% Ar/SiH_4 plasma treatment. In contrast, treatments in a 0.5 vol% doped atmosphere resulted in the formation of dense silicon layers with the sizes of particles of approximately 80 nm that covered copper surface completely. Interestingly, we could not obtain sharp images of the surfaces after Ar/SiH_4 plasma treatment in 0.05 vol% and 0.1 vol% atmospheres (c.f. Fig. 3c, d). We assumed

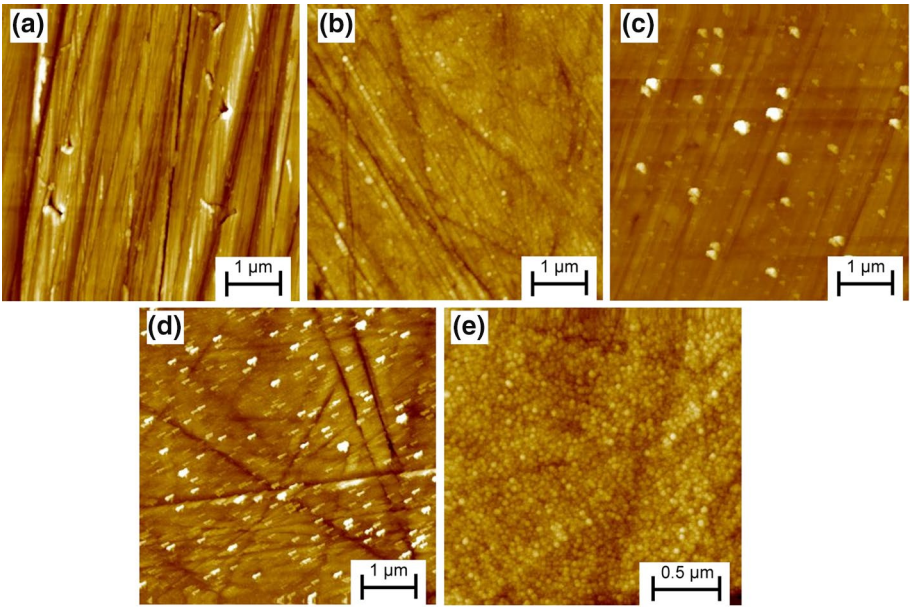

Fig. 3 AFM images of the samples after 10 s of Ar (**a**), 0.02% SiH_4 in Ar (**b**), 0.05% SiH_4 in Ar (**c**), 0.1% SiH_4 in Ar (**d**) and 0.5% SiH_4 in Ar (**e**) plasma treatments. The scan size is 5×5 µm, except for (**e**), which is shown at the scan size of 2×2 µm

that deposited particles were loosely attached to the surfaces, so the AFM cantilever could move them along the samples. Such effect of the temporary attachment of particles to the AFM cantilever led to the effects of blurs and contributed in a deterioration of the image sharpness. Nevertheless, the obtained results provided useful information on the sizes and amount of particles. Moreover, these measurements seemed to indicate that deposited particles could be removed from surfaces mechanically (e.g. by wiping), as it is demonstrated later in the text.

In the current work, the cleaning experiment was performed on the sample that was treated for 10 s in an Ar/SiH_4 (0.05 vol%) plasma at 100 hPa and room temperature. Figure 4a shows a surface of sample after plasma treatment. As it was discussed previously, the implemented treatment resulted in the deposition of separately distributed particles on the surface. In contrast, almost no particles were observed after wiping the surface by hand in the presence of air with the precision wipes (Kimberly-Clark Worldwide, Inc., USA) for 10 s (c.f. Fig. 4b). Additionally, the absence of silicon-contained contaminations was confirmed by the XPS analysis of the sample after plasma treatment and consequent wiping in the presence of air. The concentrations of the detected species on the surface before plasma treatment, after 10 s plasma treatment and after consequent wiping are presented in the Table 2 (corresponding survey spectra are presented in the supplements, Figure S3). As it was already discussed, 10 s plasma treatment in an Ar/SiH_4 (0.05 vol%) atmosphere resulted in the strong deoxidation of copper surfaces, so an increase of copper concentration from 39.4 to 54.5 at% and the removal of oxygen species from 29.1 to 15.9 at% were detected. At the same time, deposition of silicon-contained compounds on the surface in amount of 7 at% was identified, which were not detected after the wiping procedure (c.f. Table 2). Due to the fact, that the surface was cleaned outside of the vacuum chamber in

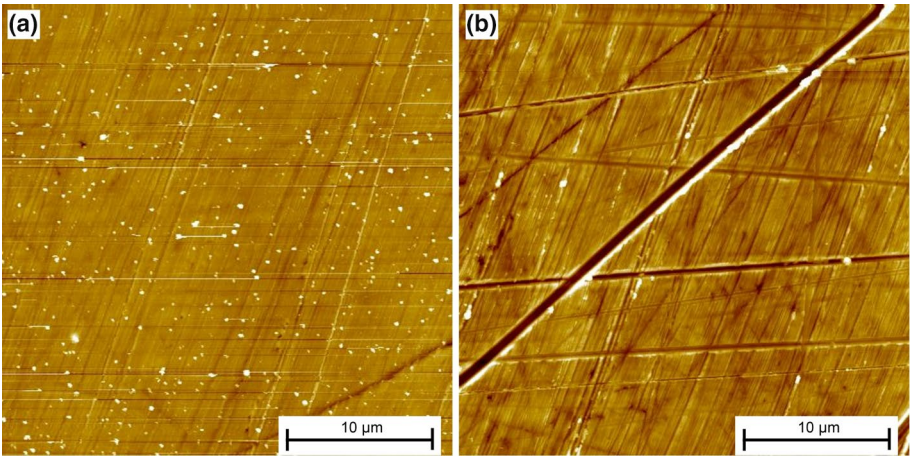

Fig. 4 AFM images of the sample after 10 s of Ar/SiH_4 (0.05 vol%) plasma treatment (**a**) and after consequent wiping (**b**). The scan size is 25 × 25 µm

Table 2 Stoichiometry (in at%) of the sample as determined with XPS for the reference state, after 10 s of Ar/SiH_4 (0.05 vol%) plasma treatment and consequent wiping

Treatment	Copper	Oxygen	Carbon	Silicon	Nitrogen
Reference	39.4	29.1	31.5	0.0	0.0
10 s plasma	54.5	15.9	21.1	7.0	1.6
Wiping	56.5	24.2	19.3	0.0	0.0

the presence of air, the reoxidation of copper occurred, which was observed in the XPS (c.f. Table 2, Fig. S3). The effect of reoxidation can be overcome by wiping the samples in a glove box where an oxygen-free environment like an Ar/SiH_4 atmosphere is established. It is assumed, that it could be possible to deoxidize copper surface and clean it out of deposited particles without any influence on the oxidation state. Generally, based on the performed experiments, we propose that the silicon-contained species were most probably formed in the plasma phase and physically adsorbed on the surfaces, so they could be easily removed.

Reduction Kinetics

Based on the analysis of the 10 s treatments in different SiH_4 mixtures discussed in the previous section, we performed longer treatments of copper material at the lowest concentration of silane in argon (0.02 vol%). Treatment in such atmosphere shows stronger deoxidation effect in comparison to an Ar plasma and at the same time does not result in intense deposition of silicon containing nanoparticles. The sample was treated at several time intervals from 10 to 80 s. After each time interval, it was transferred into the UHV system for a XPS analysis. The stoichiometry of sample after treatment steps was characterized by carbon, oxygen, copper, silicon and nitrogen species. Figure 5 presents the stoichiometry of the sample as a function of a treatment time. The process in general can be divided into two parts. From 0 to 30 s of treatment a sharp removal of oxygen and carbon species and increase of copper concentration are observed. This process can be assigned

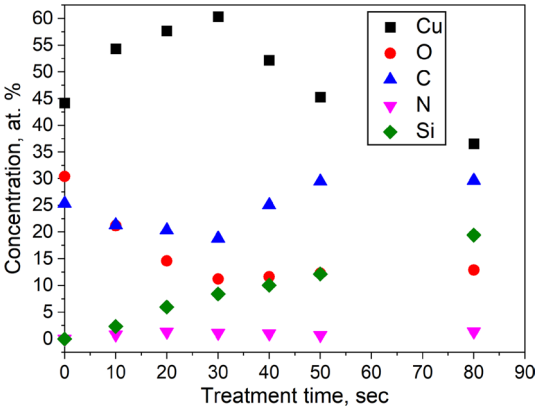

Fig. 5 Stoichiometry of the sample as a function of treatment time. The experimental data points for copper, oxygen, carbon, nitrogen and silicon species are presented in black, red, blue, pink and green colors, respectively

to the reduction of copper oxide layers and cleaning of a surface, showing a decrease of O/Cu ratio from 0.7 to 0.2. In contrast, during the first seconds more silicon particles were deposited. Thus, after 30 s of treatment we observe reduction of copper amount and increase of silicon as well as carbon concentrations. At the same time, the amount of oxygen remains on almost the same level. Such change in the behaviour could be linked with the deposition of silicon and silicon oxide particles on the metal surface that results in the decrease of intensities of copper species. The increased concentration of carbon species might be related to the reaction of carbon-containing molecules with the silane species in the plasma.

We analysed the detailed XPS regions from the sample during Ar/SiH_4 plasma treatment. The Cu $2p_{3/2}$ region from the sample after plasma steps was identified with almost similar structure, showing one sharp peak of Cu/Cu_2O components at the binding energy value of 932.6 eV [41, 47] (shown in the supplements, Figure S4). The reference sample was characterized by the slightly asymmetrical Cu/Cu_2O peak at 932.4 eV and the low-intensity shake-up structure (c.f. Fig. S4). The presence of asymmetry and the low-intensity shake-up structure provides the possibility to estimate the nature and amount of Cu^{2+} species that were present on the surface before treatment [8, 28, 41, 43, 47, 48]. The fitting of the Cu $2p_{3/2}$ detailed region revealed that the native oxide layer of the reference sample was mainly composed of Cu_2O oxide with minor addition of $Cu(OH)_2$, which signals were detected at 932.4 and 934.7 eV, respectively [28, 29, 48]. The ratio of Cu_2O/Cu to $Cu(OH)_2$ species was approximately 0.88 to 0.12 before plasma treatment and 1.00 to 0.00 already after 10 s of the implemented plasma treatment.

An illustrative example of almost full reduction of copper native oxide layers in an Ar/SiH_4 atmosphere by using a sub-atmospheric DBD plasma is shown in the Fig. 6a, b. The copper Auger region (c.f. Fig. 6a) before plasma treatment (bottom spectrum, dark green line) is characterized by two main spectroscopic lines of Cu and Cu_2O at 568 and 569.8 eV, respectively. Already after 10 s of treatment a slight increase of the intensity of a Cu line and decrease of a Cu_2O line were observed. The typical structure of a Cu LMM spectrum of a clean copper sample was observed after 50 s of treatment (c.f. Fig. 6a, orange line), showing highly intense Cu line at 568 eV [41].

A reduction of copper oxide was also observed in the O 1 s region during treatment (c.f. Fig. 6b). That is, the O 1 s spectrum from the sample before treatment (bottom line) was composed of three main components as lattice Cu_2O oxide, adsorbed surface

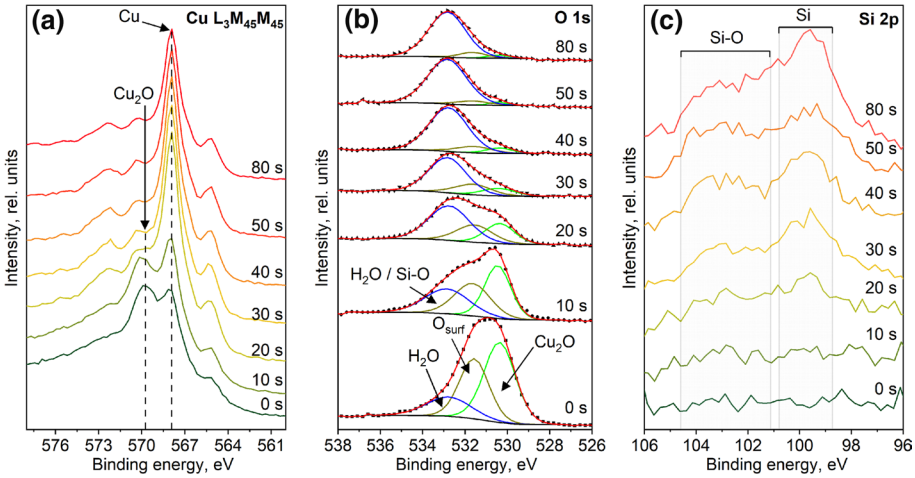

Fig. 6 **a** Cu $L_3M_{45}M_{45}$, **b** O 1 s and **c** Si 2p regions of reference sample (bottom line) and after 10 to 80 s plasma treatment in an Ar/SiH_4 (0.02 vol%) gas (spectra are displayed from bottom to top)

oxygen species (like OH^- groups) and molecular water as well as oxygen-containing organic species (like C–O–C and O–C=O) at 530.5, 531.7 and 532.9 eV, respectively [9, 28, 41, 43]. The intensity of Cu_2O as well as surface oxygen components decreased after each treatment step, showing almost no signal after approximately 50–80 s of treatment. At the same time, the intensity of a component at the higher binding energy of 532.9 eV started to increase after 10 s of treatment that can be linked with the deposition of oxidized Si–O particles on the surface. According to literature, Si–O species as well as water and organic carbon components are expected to be present in the O 1 s region at almost the same binding energies in the range from 532.2 to 533.5 eV [9, 37, 41, 43–46]. Therefore, in the current publication it was concluded to assign all of these components to one broad peak at 532.9 eV.

The process of deposition of silicon and silicon oxide particles on the surface was observed within the Si 2p detailed spectra from the copper sample during treatment (c.f. Fig. 6c). Taking into account the minor presence of nitrogen on the surface of approximately 1 at% and major amount of oxygen during treatment, we simplified the analysis of the detailed Si 2p region to the characterization of oxidized silicon species only. Therefore, the Si 2p region from the sample during treatment was divided into two parts. The first part in the binding energy range from 99 to 101 eV is characterized by a wide Si^0 structure. The second part in the range from 101 to 104 eV was assumed to be the superposition of the emissions from different states of silicon in the oxidized forms (Si–O, with Si^{1+}, Si^{2+}, Si^{3+} and Si^{4+}). As it was observed, a minor amount of Si–O species were deposited in the first 10 s of treatment. An increase of intensities of the emission peaks of Si and Si–O started to be seen after 20 s of treatment, showing their maximum after 80 s. Table 3 presents the XPS results for the reference Cu sample and after 80 s of Ar/SiH_4 plasma treatment. Relative fraction of copper native oxide layer was reduced from 48 to 3% after 80 s of treatment. This result shows that the implemented plasma method can be used for the reduction of copper oxides.

Table 3 XPS results for the reference Cu sample and after 80 s of Ar/SiH_4 (0.02 vol%) plasma treatment

System	Peak	Species	Binding energy, eV	FWHM, eV	Relative fraction, %
Reference sample	C 1 s	C–C, C–H	285.0	1.6	62
		C–O	286.2	1.9	20
		C=O	288.5	2.0	18
	O 1 s	Cu_2O	530.5	1.8	50
		O_{surf}	531.7	1.6	34
		H_2O	532.9	2.5	16
	Cu 2p	Cu_2O/Cu	932.4	1.7	88
		$Cu(OH)_2$	934.7	2.0	12
After Ar/SiH_4 plasma (80 s)	C 1 s	C–C, C–H	285.0	1.8	83
		C–O	286.2	1.9	17
		C=O	288.5	0.0	0
	O 1 s	Cu_2O	530.5	1.6	4
		O_{surf}	531.7	1.5	3
		H_2O/Si–O	532.9	2.2	93
	Si 2p	Si–Si $2p_{3/2}$	99.3	2.0	34
		Si–Si $2p_{1/2}$	99.9	1.3	17
		Si_2O	101.0	1.3	1
		SiO	101.3	1.5	15
		Si_2O_3	102.4	1.1	6
		SiO_2	103.6	2.0	27
	Cu 2p	Cu_2O/Cu	932.6	1.6	100

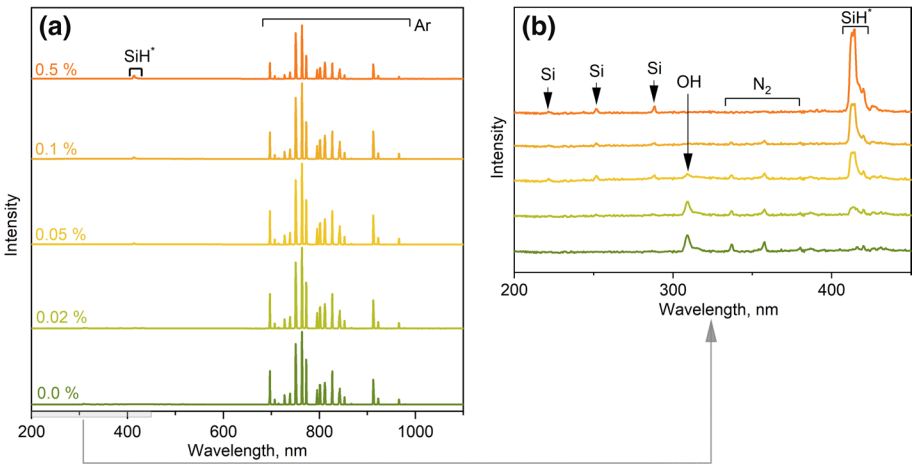

Fig. 7 OES spectra of the plasma phases in the wavelength ranges of **a** 200–1100 nm and **b** 200–450 nm

Characterization of the Reactive Species in Plasma

Figure 7 displays OES spectra of Ar/SiH_4 plasmas with the concentration of silane from 0.0 to 0.5 vol%. We show that pure Ar plasma is mainly characterized by highly intense emission lines of Ar reactive species in the region from 694 to 980 nm [49, 50]. Moreover, additional low intense lines were observed in the wavelength range from 300 to 400 nm. Signal at 310 nm was assigned to hydroxyl radicals (OH) [50–52], whereas other lines at 337, 358 and 380 nm were assumed to be emissions from nitrogen N_2 species [50–52] (c.f. Fig. 7b), which are typical contaminations in argon gases [35, 51]. In contrast, SiH_4-doped argon plasmas show additional emission peak at 414 nm that is enlarged with the increase of a SiH_4 concentration. This line was associated with SiH^* radical, which is usually observed in silane plasmas [26, 27, 53]. Additionally, we observed a gradual decrease of intensities of the lines from OH radicals and N_2 species with an increase of SiH_4 concentration (a semi-quantitative comparison of intensities of SiH^*, Si, OH and N_2 lines in relation to the main Ar line for different silane concentrations are presented in Figure S5 in supplements). Therefore, it can be assumed that silane molecules react with residual nitrogen and oxygen contaminations in an Ar gas that resulted in deposition of Si–O as well as Si–N species on the treated surfaces. Interestingly, no emissions from H_α were observed in SiH_4-doped Ar plasmas like it was detected in several studies on highly-concentrated SiH_4 plasmas [26, 53]. Therefore, the OES analysis indicates that the deoxidation effect of Ar/SiH_4 plasmas observed in XPS can be assigned to the presence of SiH^* radicals and the corresponding elimination of residual oxygen as well as nitrogen species in an Ar gas.

Conclusions

The deoxidation effect of a DBD plasma in a promising protective atmosphere of Ar/SiH_4 at 100 hPa and room temperature was studied. It is shown that an addition of a SiH_4 gas to an Ar atmosphere results in the increase of the deoxidation effect of an Ar DBD plasma. That is, even minor addition of silane to an Ar gas in the amount of 0.02 vol% leads to much more effective reduction of copper surface oxides after 10 s treatment in comparison to a pure Ar plasma. Moreover, by increasing the silane concentration up to 0.1 vol% the deoxidation effect of a DBD plasma can be improved, so almost no Cu_2O native oxide can be observed on the surface after 10 s treatment. Treatment for longer times also improves the deoxidation effect, so oxide layers can be almost fully reduced after 80 s of treatment in an Ar/SiH_4 gas at the lowest concentration of 0.02 vol%. At the same time, an addition of a silane gas to the mixture results in deposition of silicon-containing particles such as pure silicon as well as Si^{x+} (with Si^{1+}, Si^{2+}, Si^{3+} and Si^{4+}) species in a form of oxides and nitrides on the surface. For instance, 10 s DBD plasma treatment in an Ar/SiH_4 (0.02 vol%) atmosphere shows a formation of a minor amount of Si-contained species as particles with a diameter of 80 nm. With the increase of the concentration up to 0.1 vol% more Si, Si–O and Si–N particles with a diameter of 200–300 nm are observed. Treatment for 10 s in an Ar/SiH_4 with the silane concentration of 0.5 vol% shows formation of a homogeneous > 10 nm-thick layer of non-oxidized Si on Cu surface. Despite the fact, that the process of deoxidation in such atmospheres involved deposition of Si and Si^{x+} species on the surface, it is shown that the contaminations can be removed from the treated copper surfaces by wiping. Additionally, the plasma phase at different SiH_4 concentrations was studied and

it was observed that the deoxidation effect of the implemented method coincides with the presence of SiH^* radicals, whereas no atomic hydrogen radicals H_α were observed. Moreover, an elimination of Ar gas contaminations, which were presented in the OES spectra as OH radicals and N_2 species, by addition of a SiH_4 gas was observed.

Supplementary Information The online version contains supplementary material available at https://doi.org/10.1007/s11090-022-10268-w.

Acknowledgments The project was funded by the Deutsche Forschungsgemeinschaft (DFG, German Research Foundation)—Project-ID 394563137—SFB1368.

Author's Contribution V. Udachin: Conceptualization, Formal analysis, Investigation, Data Curation, Writing—Original Draft, Visualization. L. Wegewitz: Conceptualization, Writing—Original Draft. S. Dahle: Conceptualization, Formal analysis, Data Curation, Writing—Original Draft, Funding acquisition. W. Maus-Friedrichs: Conceptualization, Resources, Writing—Review & Editing, Supervision, Project administration, Funding acquisition.

Funding Open Access funding enabled and organized by Projekt DEAL.

Data Availability Statement All raw and analyzed data have been made available through Zenodo at https://doi.org/10.5281/zenodo.6078060.

Declarations

Conflict of Interest The authors have no relevant financial or non-financial interests to disclose.

References

1. Yabuki A, Arriffin N (2010) Electrical conductivity of copper nanoparticle thin films annealed at low temperature. Thin Solid Films 518:7033–7037. https://doi.org/10.1016/j.tsf.2010.07.023
2. Pai P-L, Ting CH (1989) Selective electroless copper for VLSI interconnection. IEEE Electron Device Lett 10:423–425. https://doi.org/10.1109/55.34730
3. Sawada Y, Ogawa S, Kogoma M (1995) A new approach to the copper/epoxy joint using atmospheric pressure glow discharge. J Adhes 53:173–182. https://doi.org/10.1080/00218469508009937
4. Sawada Y, Tamaru H, Kogoma M et al (1996) The reduction of copper oxide thin films with hydrogen plasma generated by an atmospheric-pressure glow discharge. J Phys D: Appl Phys 29:2539–2544. https://doi.org/10.1088/0022-3727/29/10/003
5. Di L, Zhang X, Xu Z (2014) Preparation of copper nanoparticles using dielectric barrier discharge at atmospheric pressure and its mechanism. Plasma Sci Technol 16:41–44. https://doi.org/10.1088/1009-0630/16/1/09
6. Sawada Y, Taguchi N, Tachibana K (1999) reduction of copper oxide thin films with hydrogen plasma generated by a dielectric-barrier glow discharge. Jpn J Appl Phys 38:6506–6511. https://doi.org/10.1143/JJAP.38.6506
7. Xu ZJ, Qi B, Di LB (2013) On the mechanism of copper oxide reduction by dielectric barrier discharge plasma using H_2 and Ar mixture gases. AMR 690–693:1664–1667. https://doi.org/10.4028/www.scientific.net/AMR.690-693.1664

8. Prysiazhnyi V, Brablec A, Čech J et al (2014) Generation of large-area highly-nonequlibrium plasma in pure hydrogen at atmospheric pressure. Contrib Plasma Phys 54:138–144. https://doi.org/10.1002/ctpp.201310060
9. Udachin V, Wegewitz L, Dahle S et al (2022) Reduction of copper surface oxide using a sub-atmospheric dielectric barrier discharge plasma. Appl Surf Sci 573:151568. https://doi.org/10.1016/j.apsusc.2021.151568
10. Ramos SV, Cisquini P, Nascimento RC Jr et al (2021) Morphological changes and kinetic assessment of Cu2O powder reduction by non-thermal hydrogen plasma. J Mark Res 11:328–341. https://doi.org/10.1016/j.jmrt.2020.12.038
11. Lee SY, Mettlach N, Nguyen N, Sun YM, White JM (2003) Copper oxide reduction through vacuum annealing. Appl Surf Sci 206:102–109. https://doi.org/10.1016/S0169-4332(02)01239-4
12. Lynch S (2012) Hydrogen embrittlement phenomena and mechanisms. Corros Rev. https://doi.org/10.1515/corrrev-2012-0502
13. Woodtli J, Kieselbach R (2000) Damage due to hydrogen embrittlement and stress corrosion cracking. Eng Fail Anal 7:427–450. https://doi.org/10.1016/S1350-6307(99)00033-3
14. Gangloff RP, Wei RP (1977) Gaseous hydrogen embrittlement of high strength steels. Metall Mater Trans A 8:1043–1053. https://doi.org/10.1007/BF02667388
15. Holländer U, Wulff D, Langohr A et al (2019) Brazing in SiH4-doped inert gases: a new approach to an environment friendly production process. Int J Precis Eng and Manuf-Green Tech. https://doi.org/10.1007/s40684-019-00109-1
16. Gustus R, Szafarska M, Maus-Friedrichs W (2021) Oxygen-free transport of samples in silane-doped inert gas atmospheres for surface analysis. J Vac Sci Technol, B: Nanotechnol Microelectron: Mater, Process, Meas, Phenom 39:54204. https://doi.org/10.1116/6.0001180
17. Emminghaus N, Fritsch S, Büttner H et al (2021) PBF-LB/M process under a silane-doped argon atmosphere: preliminary studies and development of an innovative machine concept. Adv Ind Manufact Eng 2:100040. https://doi.org/10.1016/j.aime.2021.100040
18. Maier HJ, Herbst S, Denkena B et al (2020) Towards dry machining of titanium-based alloys: a new approach using an oxygen-free environment. Metals 10:1161. https://doi.org/10.3390/met10091161
19. Kessels WMM, Severens RJ, Smets AHM et al (2001) Hydrogenated amorphous silicon deposited at very high growth rates by an expanding Ar–H2–SiH4 plasma. J Appl Phys 89:2404–2413. https://doi.org/10.1063/1.1338985
20. Yu G, Xiwen Z, Gaorong H (2007) Room temperature growth of hydrogenated amorphous silicon films by dielectric barrier discharge enhanced CVD. Plasma Sci Technol 9:177–180. https://doi.org/10.1088/1009-0630/9/2/13
21. Samanta S, Das D (2017) Nanocrystalline silicon thin films from SiH 4 plasma diluted by H 2 and He in RF-PECVD. J Phys Chem Solids 105:90–98. https://doi.org/10.1016/j.jpcs.2017.02.013
22. Parashar A, Kumar S, Dixit PN et al (2008) High-pressure condition of SiH4+Ar+H2 plasma for deposition of hydrogenated nanocrystalline silicon film. Sol Energy Mater Sol Cells 92:1199–1204. https://doi.org/10.1016/j.solmat.2008.04.008
23. Bazinette R, Paillol J, Lelièvre J-F et al (2016) Atmospheric pressure radio-frequency DBD deposition of dense silicon dioxide thin film. Plasma Process Polym 13:1015–1024. https://doi.org/10.1002/ppap.201600038
24. Jidenko N, Jimenez C, Massines F et al (2007) Nano-particle size-dependent charging and electro-deposition in dielectric barrier discharges at atmospheric pressure for thin SiO x film deposition. J Phys D: Appl Phys 40:4155–4163. https://doi.org/10.1088/0022-3727/40/14/009
25. Bazinette R, Lelièvre J-F, Gaudy L et al (2016) Influence of the discharge mode on the optical and passivation properties of SiNx: H deposited by PECVD at atmospheric pressure. Energy Procedia 92:309–316. https://doi.org/10.1016/j.egypro.2016.07.087
26. Feitknecht L, Meier J, Torres P et al (2002) Plasma deposition of thin film silicon: kinetics monitored by optical emission spectroscopy. Sol Energy Mater Sol Cells 74:539–545. https://doi.org/10.1016/S0927-0248(02)00073-9
27. van den Donker MN, Rech B, Schmitz R et al (2007) Hidden parameters in the plasma deposition of microcrystalline silicon solar cells. J Mater Res 22:1767–1774. https://doi.org/10.1557/jmr.2007.0226
28. Platzman I, Brener R, Haick H et al (2008) Oxidation of polycrystalline copper thin films at ambient conditions. J Phys Chem C 112:1101–1108. https://doi.org/10.1021/jp076981k
29. Suzuki S, Ishikawa Y, Isshiki M et al (1997) Native oxide layers formed on the surface of ultra high-purity iron and copper investigated by angle resolved XPS. Mater Trans, JIM 38:1004–1009. https://doi.org/10.2320/matertrans1989.38.1004

30. Gattinoni C, Michaelides A (2015) Atomistic details of oxide surfaces and surface oxidation: the example of copper and its oxides. Surf Sci Rep 70:424–447. https://doi.org/10.1016/j.surfrep.2015.07.001
31. Udachin V, Wegewitz L, Dahle S et al (2022) Raw and analyzed data for manuscript "Dielectric barrier discharge plasma reduction of oxidized copper surfaces in an Ar/SiH4 atmosphere." Zenodo 1:2. https://doi.org/10.5281/zenodo.6078060
32. Wegewitz L, Dahle S, Höfft O et al (2011) Plasma-oxidation of Ge(100) surfaces using dielectric barrier discharge investigated by metastable induced electron spectroscopy, ultraviolet photoelectron spectroscopy, and x-ray photoelectron spectroscopy. J Appl Phys 110:33302. https://doi.org/10.1063/1.3611416
33. Kitao A, Imakita K, Kawamura I et al (2014) An investigation into second harmonic generation by Si-rich SiN x thin films deposited by RF sputtering over a wide range of Si concentrations. J Phys D: Appl Phys 47:215101. https://doi.org/10.1088/0022-3727/47/21/215101
34. Schmid P, Orfert M, Vogt M (1998) Plasma deposition of Si-N and Si-O passivation layers on three-dimensional sensor devices. Surf Coat Technol 98:1510–1517. https://doi.org/10.1016/S0257-8972(97)00300-9
35. Mavrokoridis K, Calland RG, Coleman J et al (2011) Argon purification studies and a novel liquid argon re-circulation system. J Inst 6:P08003–P08003. https://doi.org/10.1088/1748-0221/6/08/P08003
36. Sokolov AA, Filatova EO, Afanas'ev VV et al (2009) Interface analysis of HfO2 films on (100) Si using x-ray photoelectron spectroscopy. J Phys D: Appl Phys 42:35308. https://doi.org/10.1088/0022-3727/42/3/035308
37. Dahle S, Wegewitz L, Qi F et al (2013) Silicon dioxide coating of titanium dioxide nanoparticles from dielectric barrier discharge in a gaseous mixture of silane and nitrogen. Plasma Chem Plasma Process 33:839–853. https://doi.org/10.1007/s11090-013-9472-6
38. Hollinger G, Jugnet Y, Pertosa P et al (1975) X-ray photoelectron spectroscopy of thermally grown silicon dioxide films on silicon. Chem Phys Lett 36:441–445. https://doi.org/10.1016/0009-2614(75)80276-4
39. Jakša G, Štefane B, Kovač J (2013) XPS and AFM characterization of aminosilanes with different numbers of bonding sites on a silicon wafer. Surf Interface Anal 45:1709–1713. https://doi.org/10.1002/sia.5311
40. Gritsenko VA, Kwok R, Wong H et al (2002) Short-range order in non-stoichiometric amorphous silicon oxynitride and silicon-rich nitride. J Non-Cryst Solids 297:96–101. https://doi.org/10.1016/S0022-3093(01)00910-3
41. Biesinger MC (2017) Advanced analysis of copper X-ray photoelectron spectra. Surf Interface Anal 49:1325–1334. https://doi.org/10.1002/sia.6239
42. Glaser M, Ciccullo F, Giangrisostomi E et al (2018) Doping and oxidation effects under ambient conditions in copper surfaces: a "real-life" CuBe surface. J Mater Chem C 6:2769–2777. https://doi.org/10.1039/C7TC04983H
43. Poulston S, Parlett PM, Stone P et al (1996) Surface oxidation and reduction of CuO and Cu2O studied using XPS and XAES. Surf Interface Anal 24:811–820. https://doi.org/10.1002/(SICI)1096-9918(199611)24:12%3c811:AID-SIA191%3e3.0.CO;2-Z
44. Hashemi A, Bahari A (2017) Structural and dielectric characteristic of povidone–silica nanocomposite films on the Si (n) substrate. Appl Phys A. https://doi.org/10.1007/s00339-017-1152-6
45. Kumar N, Spencer SJ, Imbraguglio D et al (2016) Extending the plasmonic lifetime of tip-enhanced Raman spectroscopy probes. Phys Chem Chem Phys 18:13710–13716. https://doi.org/10.1039/c6cp01641c
46. Trotochaud L, Head AR, Pletincx S et al (2018) Water adsorption and dissociation on polycrystalline copper oxides: effects of environmental contamination and experimental protocol. J Phys Chem B 122:1000–1008. https://doi.org/10.1021/acs.jpcb.7b10732
47. Cano E, López MF, Simancas J et al (2001) X-Ray photoelectron spectroscopy study on the chemical composition of copper tarnish products formed at low humidities. J Electrochem Soc 148:E26. https://doi.org/10.1149/1.1344547
48. Platzman I, Saguy C, Brener R et al (2010) Formation of ultrasmooth and highly stable copper surfaces through annealing and self-assembly of organic monolayers. Langmuir 26:191–201. https://doi.org/10.1021/la902006v
49. Saikia P, Saikia BK, Bhuyan H (2016) Study on the effect of hydrogen addition on the variation of plasma parameters of argon-oxygen magnetron glow discharge for synthesis of TiO 2 films. AIP Adv 6:45206. https://doi.org/10.1063/1.4947091

50. Sarani A, Nikiforov AY, Leys C (2010) Atmospheric pressure plasma jet in Ar and Ar/H2O mixtures: optical emission spectroscopy and temperature measurements. Phys Plasmas 17:63504. https://doi.org/10.1063/1.3439685
51. Knust S, Kuhlmann A, Tdl A et al (2019) Surface modification of ZnMgAl-coated steel by dielectric-barrier discharge plasma. RSC Adv 9:35077–35088. https://doi.org/10.1039/C9RA07378G
52. Rezaei F, Gorbanev Y, Chys M et al (2018) Investigation of plasma-induced chemistry in organic solutions for enhanced electrospun PLA nanofibers. Plasma Process Polym 15:1700226. https://doi.org/10.1002/ppap.201700226
53. Wang G, Shi C, Hu R et al (2015) In situ optical emission spectroscopy diagnostics of glow discharges in SiH 4 /GeH 4 /H 2. RSC Adv 5:18029–18034. https://doi.org/10.1039/C4RA17110A